Structural Durability & Health Monitoring

Tech Science Press

https://doi.org/10.32604/sdhm.2026.080529

REVIEW

Comparative Study on Temperature Actions in Structural Design Codes

Linren Zhou*, **Zhibo Xie and Jingyi Huang**

School of Civil Engineering and Transportation, South China University of Technology, Guangzhou, China

*Corresponding Author: Linren Zhou. Email: zhoulinren@scut.edu.cn

Received: 11 February 2026; Accepted: 08 April 2026; Published: 24 August 2026

ABSTRACT: Temperature action is a primary environmental load that infrastructure endures during long-term service, and it is also one of the key causes of structural performance deterioration. With global warming and the increasing frequency of extreme weather, the temperature actions on structures are becoming increasingly complex and severe. Whether current design codes can adapt to environmental climate changes, particularly regarding how to effectively respond to the impact of extreme temperatures, has become a critical concern in engineering. Based on the current structural design codes of major countries and regions (including China, the United States, New Zealand, Japan, Europe, and Hong Kong, China), this paper reviews and analyzes their calculation methods and specifications of temperature actions. The basic temperature definitions and thermal parameter selection for building structures of Chinese and European codes are compared. The requirements and distinctions regarding uniform temperature and temperature gradients in bridge design codes are analyzed. The temperature distribution characteristics for tower structures under complex solar radiation are explored. The differences in the selection of partial factors and combination values for temperature actions under the Ultimate Limit State (ULS) and Serviceability Limit State (SLS) are discussed. The study reveals that each code possesses distinct characteristics in terms of theoretical depth and engineering application. The European code establishes a refined non-linear temperature gradient model covering buildings, bridges, and towers, emphasizing the physical mechanisms of load effects and their actual engineering impact. The American code adopts a more scientific approach in limit state design by distinguishing between displacement and force effects and assigning different partial factors accordingly. The Hong Kong code (SDM), based on meteorological measurements and prediction data, has upwardly adjusted design temperature differences in response to global warming. The review and analysis of temperature actions can provide a reference for the practical application and improvement of codes in various countries, as well as an important technical basis for project owners, design units, and operation and maintenance management departments.

KEYWORDS: Structural design code; temperature action; design method; partial factor; comparative analysis

1 Introduction

According to the latest climate data released by the World Meteorological Organization (WMO), the global average surface temperature has risen by approximately 1.5°C compared to pre-industrial levels, and the warming trend continues to intensify [1]. Driven by the frequent occurrences of extreme heatwaves and intense solar radiation, both existing and newly built infrastructure are now exposed to severe temperature actions that exceed previous design standards. As a critical environmental action, temperature actions adversely impact the service performance, serviceability, durability, and safety of engineering structures, making them a key concern in current academic and engineering research [2,3].

Throughout their service life, structures are continuously exposed to complex natural environments. Due to the non-linear coupling of factors such as ambient temperature, solar radiation, and material thermal properties, the internal temperature field exhibits complex time-varying non-uniform distribution characteristics. For statically indeterminate systems, including long-span bridges [4], super-tall structures [5], and large space structures [6], the constrained non-linear thermal deformations often induce significant secondary forces. Both engineering practice and failure analyses indicate that the stress amplitude caused by thermal effects can even exceed that from live loads, making it a key factor in governing structural cracking and onset of failure [7]. Typical engineering distress cases include: cracks of prestressed concrete box-girder webs due to excessive solar temperature differentials [8], track buckling instability of ballastless tracks on high-speed railways under high temperatures [9], and joint displacements in large-span spatial steel structures caused by accumulative temperature deformations [10].

Extensive research has investigated the behavior of temperature actions and the differences in calculation models across various national codes. Hu et al. [11] addressed a limitation in Chinese specifications regarding steel box girders in cold regions; using one-year monitoring data, they demonstrated that actual vertical temperature gradients take exponential and broken-line forms, generally exceeding the specified values. Furthermore, addressing the geographical diversity of thermal actions, Cai et al. [12] conducted long-term finite element simulations across seven distinct climatic regions in China. They revealed that the singular stationary temperature gradient pattern in current Chinese codes is insufficient, proposing a region-specific model based on Extreme Value Analysis (EVA) with a 100-year return period. Based on 26 years (1999–2024) of structural health monitoring (SHM) data from the Hong Kong's Tsing Ma Bridge, Zhang et al. [13] confirmed that climate change has caused a significant rise in the bridge's annual mean temperature and extreme temperatures, at rates of 0.28°C and 0.50°C per decade, respectively. This study clearly demonstrates the long-term intensification of temperature actions on long-span bridges due to global warming. However, existing research in this field remains largely limited to individual case studies and has not systematically integrated the updated philosophy and provisions from the latest editions of major international design codes. This gap hinders a comprehensive assessment of the combined impacts of recent severe global climate change on diverse infrastructure systems.

Currently, significant disparities persist in the definitions, calculation methods, and values of partial safety factors for temperature actions across major international structural design codes, reflecting both regional practices and differing theoretical approaches. More critically, most current codes—such as the Chinese *Load Code for the Design of Building Structures* (GB 50009-2012) [14] and *General Specifications for Design of Highway Bridges and Culverts* (JTG D60-2015) [15], the European Norm (EN 1991-1-5:2003) [16], and the American *AASHTO LRFD Bridge Design Specifications* (2024) [17]—often rely on historical climatic data that fail to adequately account for the recent acceleration of global warming. This reliance on outdated baselines raises substantial safety concerns due to potentially understated design loads. In response, the Hong Kong (China) *Structures Design Manual for Highways and Railways* (SDM) [18] implemented a significant revision in 2023, substantially increasing the design temperature differentials to address climate change. This revision demonstrates and sets a necessary precedent for code modernization.

Therefore, this study conducts a systematic review and comparative analysis of temperature actions in structural design, aiming to clarify the similarities, differences, and underlying reasons in the computational logic and theoretical basis of various national codes. The following design codes were selected for comparative analysis: the Chinese JTG [15,19]/GB [14,20,21]/TB [22] system, the American AASHTO LRFD [17], the New Zealand NZTA [23], the Japanese JSHB [24], the European EN 1991-1-5 [16], and the Hong Kong (China) SDM [18]. These codes cover diverse infrastructure types, including building structures, bridge engineering, high-rise structures, and steel structures. The comparative analysis focuses on discrepancies in defining the base temperature, determining the effective temperature, and modeling non-linear temperature gradients across these codes. Furthermore, it analyzed the strategies employed for selecting partial safety factors and combination values under limit states. The findings provide a reference for future revisions of structural design codes and offer guidance for practical engineering design.

While temperature-induced actual structural effects are practically crucial, they are highly sensitive to specific bridge typologies, cross-sectional dimensions, and boundary conditions. Therefore, to maintain a generalized and macroscopic perspective, this review focuses primarily on evaluating the fundamental discrepancies and theoretical evolution of the normative temperature models themselves. Comprehensive quantitative structural response evaluations based on these updated codes will be the focus of our future research.

2 Comparative Analysis of Temperature Actions for Building Structures

Temperature actions on building structures are primarily attributed to uniform thermal expansion/contraction from ambient air temperature changes and non-uniform temperature gradients induced by solar radiation. As the Chinese and European codes have developed relatively detailed and representative design provisions for temperature actions in buildings, this section focuses on a comparative analysis between them. While sharing a common logical framework, the two codes exhibit significant differences in the specified values of key parameters.

2.1 Definition of Reference Temperature

The reference temperature serves as the fundamental meteorological parameter for determining temperature actions. An essential distinction exists between the two codes regarding its definition:

(1) Chinese Code (GB 50009)

This code utilizes the monthly mean maximum ($T_{\max}$) and minimum ($T_{\min}$) air temperatures with a 50-year return period. This approach smooths out transient extreme temperatures and primarily reflects seasonal variations.

(2) European Code (EN 1991-1-5)

This code employs the hourly mean maximum ($T_{\max}$) and minimum ($T_{\min}$) air temperatures with a 50-year return period. This method is more capable of capturing the increasingly frequent fluctuations of extreme temperatures under global warming.

2.2 Uniform Temperature Action

The uniform temperature action primarily induces overall expansion and contraction of the structure. Both codes employ calculation models based on the temperature difference, ΔT:

(1) Chinese Code (GB 50009)

This code emphasizes an allowable range for the initial temperature (closure temperature). The maximum temperature rise and drop are determined as the difference between the structure's highest/lowest mean temperature and the lowest/highest initial temperature, as defined by Eqs. (1) and (2). For structures with significant temperature differences between indoor and outdoor environments, the structural mean temperature must be determined in accordance with heat transfer principles.

Maximum temperature rise:

$$\Delta T_{\mathrm{k}} = T_{\mathrm{s,max}} - T_{0,\mathrm{min}} \tag{1}$$

Maximum temperature drop:

$$\Delta T_{\mathrm{k}} = T_{\mathrm{s,min}} - T_{0,\mathrm{max}} \tag{2}$$

where ΔT_{k} is the characteristic value of the uniform temperature action (°C); $T_{\mathrm{s,max}}$ and $T_{\mathrm{s,min}}$ are the maximum and minimum mean temperatures of the structure (°C), respectively; $T_{0,\mathrm{max}}$ and $T_{0,\mathrm{min}}$ are the maximum and minimum initial mean temperatures of the structure (°C), respectively.

(2) European Code (EN 1991-1-5)

This code explicitly accounts for the influence of different seasonal initial temperatures—winter vs. summer construction—on the uniform temperature difference, as expressed in Eq. (3):

$$\Delta T = T - T_0 \tag{3}$$

where T is the mean temperature of the structure; T_0 is the initial temperature.

2.3 Non-Uniform Temperature Difference

In addition to the uniform temperature variations described above, building structures are subjected to a complex non-uniform temperature field influenced by differences between indoor and outdoor environments, solar radiation, and the soil thermal properties.

2.3.1 Temperature of the Inner Environment

The indoor environmental temperature is a key parameter for determining the thermal boundary condition at the interior surface of the structure. Its value depends primarily on the building's intended use, the HVAC (Heating, Ventilation, and Air Conditioning) system, and the distribution of internal heat sources.

(1) Chinese Code (GB 50009)

This code adopts a project-specific analytical approach, prioritizing the use of architectural design data for determination. In the absence of such data, it is recommended to consider unfavorable conditions under summer air conditioning and winter heating scenarios. The code does not provide unified numerical recommendations, which offers design flexibility but lacks prescriptive guidance during the preliminary design stage.

(2) European Code (EN 1991-1-5)

This code provides prescriptive recommended values. For conventional buildings, it suggests adopting an indoor temperature of 20°C in summer and 25°C in winter, facilitating rapid estimation in engineering practice.

2.3.2 Temperature of Outdoor Above-Ground Structures

Above-ground structures exposed to the external environment are subjected to the combined effect of short-wave solar radiation and long-wave environmental radiation. Consequently, their surface temperature is often significantly higher than the ambient air temperature and exhibits pronounced non-uniformity due to factors such as orientation and the thermal properties of the surface material.

(1) Chinese Code (GB 50009)

This code adopts a tabular approach to determine the temperature increment, which is directly added to the maximum air temperature. The increment value is determined based on the orientation of the structure and its surface colour, with specific values provided in Table 1. This method facilitates manual calculation but does not account for seasonal variations or the influence of thermal parameters.

Table 1: Temperature increase of enclosure structure surfaces considering solar radiation in Chinese code.

Orientation	Surface Colour	Temperature Increment (°C)
Flat roof	Bright light	6
	Light colour	11
	Dark	15
Vertical walls facing east, south, and west	Bright light	3
	Light colour	5
	Dark	7
Vertical walls facing north, northeast, and northwest	Bright light	2
	Light colour	4
	Dark	6

(2) European Code (EN 1991-1-5)

This code introduces the concept of relative absorptivity and distinguishes between seasons, thereby providing a clearer physical significance, as illustrated in Table 2. The most notable difference lies in the sensitivity to orientation. In the Chinese code, the temperature increment for sun-exposed surfaces (east, south, and west) differs only slightly from that for shaded surfaces (north, northeast, and northwest), typically by just 1°C–2°C. In contrast, the European code shows a substantially greater disparity: the extreme temperature difference between surfaces with high solar gain (south, southwest, and west) and those with low solar gain (north, northeast, and east) can exceed 30°C. This indicates that the European code assesses the heat effect of direct solar radiation far more stringently than its Chinese counterpart.

Table 2: Maximum temperature of outdoor above-ground structures in Eurocode.

Orientation	Season	Relative Absorptivity	Temperature (°C)
North, northeast, and east orientation	Summer	0.5 bright light surface	$T_{\max} + 0$
		0.7 light coloured surface	$T_{\max} + 2$
		0.9 dark surface	$T_{\max} + 4$
		Winter	$T_{\min}$
South, southwest, and west orientations	Summer	0.5 bright light surface	$T_{\max} + 18$
		0.7 light coloured surface	$T_{\max} + 30$
		0.9 dark surface	$T_{\max} + 42$
		Winter	$T_{\min}$

Note: Numerical values in the table are recommended values.

2.3.3 Temperature of Outdoor Underground Structures

Underground structures are influenced by the soil thermal inertia. This thermodynamic difference between above-ground and subsurface environments often leads to significant vertical temperature gradient effects within the structural system.

(1) Chinese Code (GB 50009)

For depths exceeding 10 m below ground surface, the soil is generally considered to be in a constant-temperature regime. The temperature is taken as the local annual mean air temperature. It should be explicitly noted that this numerical assumption—a constant temperature boundary at a depth of 10 m—is primarily applicable to the foundations of conventional buildings and bridges under normal environmental conditions, which strictly delineates the scope of this comparative study.

(2) European Code (EN 1991-1-5)

In contrast, greater attention is given to the temperature gradient in shallow soil layers, with specific seasonal recommended values provided:

Summer: 8°C for depths < 1 m; 5°C for depths > 1 m.

Winter: −5°C for depths < 1 m; −3°C for depths > 1 m.

3 Comparison of Temperature Actions on Bridge Structures

As most bridges are exposed, statically indeterminate systems, they are particularly sensitive to thermal effects. The differences among national codes in this field are primarily reflected in their respective approaches to modeling vertical temperature gradients.

The nominal temperature values across national codes originate from fundamentally different statistical baselines. The Eurocode and Chinese GB 50009 establish a probabilistic framework, utilizing a 50-year return period based on the Type I extreme value (Gumbel) distribution. In contrast, AASHTO LRFD aligns environmental loads with a 75-year design life; its Procedure B directly adopts absolute extremes from a 70-year meteorological history rather than a probability density function, while Procedure A relies on empirical envelopes. Similarly, the NZTA and JSHB codes apply deterministic regional envelopes.

Because codes like AASHTO, NZTA, and JSHB are empirically governed, mathematically normalizing these values to a single probabilistic baseline (e.g., a 50-year return period) is unfeasible without raw local meteorological variance data. Therefore, the values compared herein represent the ultimate jurisdictional "design envelopes"—blending probabilistic models and historical extremes—rather than strictly equivalent statistical parameters.

3.1 Closure Temperature in Bridge Design

For statically indeterminate bridges, the uniform temperature change that induces secondary internal forces cannot be determined without establishing a stress-free baseline, known as the closure temperature. During the design phase, different codes adopt varying strategies to define this critical reference point.

(1) European Code (EN 1991-1-5)

The Eurocode explicitly defines the "initial temperature" as the temperature of a structural element at the relevant stage of its restraint. To address uncertainties during the design phase when the exact construction schedule is unknown, the code recommends using the average temperature during the construction period. If no such information is available, a default value of 10°C is recommended.

(2) American Code (AASHTO LRFD)

The AASHTO specifications refer to this baseline as the "setting temperature" or "base construction temperature." It is defined as a structure's average temperature used to determine dimensions when a component is added or set in place.

(3) Chinese Codes (JTG D60 and TB 10002)

The Chinese highway bridge code (JTG D60) specifies that the calculation of structural deformations or restraint forces must start from the "structural temperature when it is restrained". The railway bridge code (TB 10002) explicitly terms this the "temperature at the time of closure".

3.2 Uniform Temperature Action

Uniform temperature action induces longitudinal expansion and contraction of bridges, which governs the design of expansion joints and piers. Herein, the terms "standard value" and "characteristic value" equivalently represent the unfactored thermal action across different codes.

(1) American Code (AASHTO LRFD)

This code provides two alternative calculation procedures with specified applicability.

Procedure A is based on historical practice. It directly prescribes the extreme design temperature differences (upper and lower limits) according to climate zones (moderate or cold) and material types (steel, concrete, or wood), as shown in Table 3. This procedure is applicable to all bridge types.

Table 3: Design temperature ranges for AASHTO procedure A in US code (°C).

Climate	Steel or Aluminum		Concrete		Wood	
	Maximum	Minimum	Maximum	Minimum	Maximum	Minimum
Cold	49	−34	27	−18	24	−18
Moderate	49	−18	27	−12	24	−12

Unit Conversion Note: The environmental temperatures and structural dimensions prescribed in the AASHTO LRFD specifications are originally defined in US Customary Units (Fahrenheit °F and inches in). To facilitate a direct and intuitive cross-code comparison, all AASHTO values presented in this table/figure have been analytically converted to the International System of Units (Celsius °C and millimeters mm).

Procedure B is based on the research by Roeder (2002). It utilizes 70 years of recorded meteorological data to develop isotherm maps, from which the maximum and minimum design temperatures can be determined directly. However, it is applicable only to concrete girder bridges or steel girder bridges with a concrete deck.

(2) Chinese Code (JTG D60)

This code adapts Calculation Procedure A from the AASHTO specifications, with modifications to account for China's geographical and climatic characteristics. It divides the country into three climatic zones: severe cold, cold, and moderate. For each zone, the code specifies the maximum and minimum effective temperatures for different types of bridge deck surfacing, with the specific values provided in Table 4.

Table 4: Standard values of effective temperature for highway bridges in Chinese code (°C).

Climate	Steel Bridges with Steel Decks		Steel Bridges with Concrete Decks		Concrete Bridges and Masonry Bridges	
	Maximum	Minimum	Maximum	Minimum	Maximum	Minimum
Severe cold	46	−43	39	−32	34	−23
Cold	46	−21	39	−15	34	−10
Moderate	46	−9 (−3)	39	−6 (−1)	34	−3 (0)

Note: The values in parentheses apply to the Kunming, Nanning, Guangzhou, and Fuzhou regions.

(3) New Zealand Code (NZTA)

Owing to the country's generally moderate climate and climatically uniform conditions, this code specifies the characteristic values of the uniform temperature difference as ±25°C for steel structures and ±20°C for concrete structures.

(4) Japanese Code (JSHB)

Based on geographical latitude and climatic characteristics, this code divides the design territory into cold and mild regions. Accordingly, it specifies reference temperature and effective temperature for structures, with detailed values provided in Table 5.

Table 5: Design temperature parameters for highway bridges in Japanese code.

Temperature Parameters		Cold Region	Mild Region
Reference temperature		+20 °C	+10 °C
Effective temperature	Steel structures	−30°C~ +50 °C	−10°C~ +50 °C
	Concrete structures	The characteristic value of the overall structural temperature difference is taken as +15°C. If the minimum dimension of the cross section is 700 mm or more, the value is reduced to +10°C.	

(5) European Code (EN 1991-1-5)

Based on deck material, this code classifies bridges into three types: bridges with steel decks, bridges with composite decks, and bridges with concrete decks. It establishes a linear conversion relationship between the shade air temperatures ($T_{\max}$, $T_{\min}$) and the corresponding uniform bridge temperature components ($T_{e,\max}$, $T_{e,\min}$), as illustrated in Fig. 1.

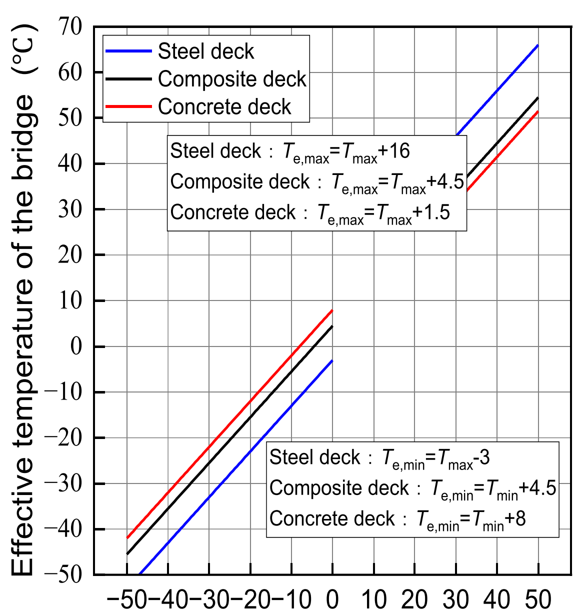

Figure 1: Correlation between minimum/maximum air temperature ($T_{\min}/T_{\max}$) and minimum/maximum effective bridge temperature ($T_{e,\min}/T_{e,\max}$) in Eurocode.

(6) Hong Kong Code (SDM)

The Structures Design Manual for Highways and Railways (SDM) issued by the Highways Department follows the framework of the European code but introduces further distinctions between normal structures and minor structures. To determine the minimum and maximum uniform bridge temperatures ($T_{\mathrm{e,min}}$ and $T_{\mathrm{e,max}}$), designers may directly refer to the values provided in the code, bypassing the meteorological data conversion calculations required by the European code. This simplified approach reflects Hong Kong's limited geographical area and relatively uniform climate.

In a proactive response to global warming, the Hong Kong (China) code implemented a forward-looking adjustment in its 2023 revision. Compared to the 2013 edition, the 2023 code maintains the minimum uniform bridge temperature ($T_{\mathrm{e,min}}$) at 0°C while significantly raising the values for the maximum uniform bridge temperature ($T_{\mathrm{e,max}}$), as detailed in Table 6. The upward adjustments for all deck types are approximately 20%. Notably, the increase for concrete decks is the largest in relative terms: from 36°C to 45°C, representing a 25.0% increase. Conversely, steel decks exhibit the greatest absolute rise: from 46°C to 55°C—a net increase of 9°C, corresponding to a relative increase of 19.6%. These revisions to the Hong Kong code, particularly the significant elevation of the maximum uniform bridge temperature, directly underscore the growing challenge that climate change poses to infrastructure through intensified temperature actions.

Table 6: Comparative analysis of maximum design temperatures ($T_{\mathrm{e,max}}$) in Hong Kong code 2013 and 2023 editions.

Superstructure Type	Structure Importance	The Code's 2013 $T_{\mathrm{e,max}}$ Value (°C)	The Code's 2023 $T_{\mathrm{e,max}}$ Value (°C)	Absolute Increment ΔT (°C)	Increase Range (%)
Steel deck	Normal structures	46	55	+9	19.6
	Minor structures	44	53	+9	20.5
Composite beam bridge deck	Normal structures	40	48	+8	20.0
	Minor structures	38	46	+8	21.1
Concrete deck	Normal structures	36	45	+9	25.0
	Minor structures	34	43	+9	26.5

While the Hong Kong code (2025 Revision) commendably elevates design temperatures using updated meteorological data—typically employing traditional stationary Extreme Value Theory (EVT)—this adjustment remains a deterministic patch. Global warming induces climate non-stationarity, invalidating the conventional assumption that historical extreme frequencies can reliably predict future probabilities. To scientifically address this, future structural codes must transition to Non-Stationary Extreme Value Theory (NS-EVT). In an NS-EVT framework, the parameters of extreme value distributions (e.g., location μ and scale σ) are not constants, but time-varying functions or covariates explicitly linked to climate projection models. This dynamic probabilistic approach is essential for maintaining structural reliability over the design life cycle in a rapidly warming environment.

3.3 Vertical Temperature Gradient

The vertical temperature gradient in bridges, induced by the attenuation of solar radiation through the cross-section depth, is a primary cause of secondary moments in the main girders and self-equilibrating stresses.

(1) American Code (AASHTO)

This code models the vertical temperature gradient using either a bi-linear or tri-linear pattern, as shown in Fig. 2. The United States is divided into four zones, each with specified base temperatures T_1 and T_2, detailed in Table 7. Unless a site-specific investigation is conducted, the temperature value T_3 shall be taken as 0°C, but in no case shall it exceed 3°C. For negative temperature gradients, the code specifies that the positive gradient values be multiplied by the following reduction factors: −0.30 for plain concrete decks and −0.20 for decks with an asphalt overlay.

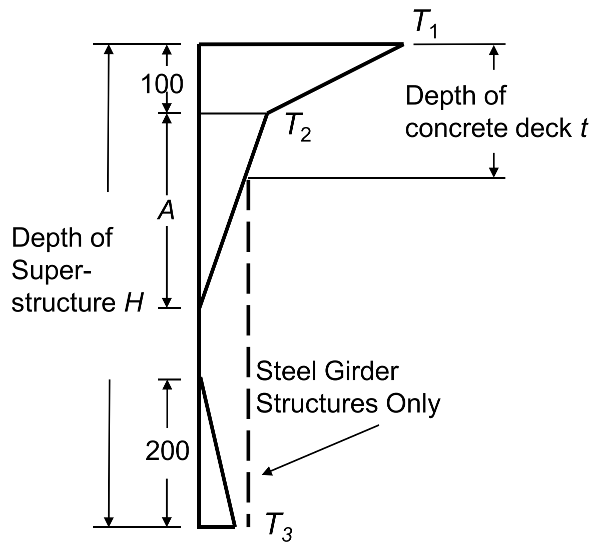

Figure 2: Vertical temperature gradient model in AASHTO code (unit: mm). Note: For concrete structures, A = 300 mm when the girder depth is greater than or equal to 400 mm; A = 100 mm when the girder depth is less than 400 mm, and in the latter case, A shall not exceed the actual thickness. For steel girders with a concrete deck, A = 300 mm, where t is the thickness of the concrete deck.

Table 7: Temperature basis for vertical solar positive temperature difference in AASHTO code.

Zone	T_1 (°C)	T_2 (°C)
1	30	7.8
2	25.6	6.7
3	22.8	6.1
4	21.1	5.0

Unit Conversion Note: The environmental temperatures and structural dimensions prescribed in the AASHTO LRFD specifications are originally defined in US Customary Units (Fahrenheit °F and inches in). To facilitate a direct and intuitive cross-code comparison, all AASHTO values presented in this table/figure have been analytically converted to the International System of Units (Celsius °C and millimeters mm).

(2) Chinese Code (JTG D60)

This code adopts the bi-linear pattern for the vertical temperature gradient from the American specifications, as illustrated in Fig. 3. Departing from the zoning approach, it specifies the temperature difference at the top surface (T_1) according to the type of deck surfacing, as provided in Table 8. For negative temperature gradients, a more conservative and simplified approach is applied: a uniform reduction factor of

−0.5 is applied to the positive temperature gradients. This factor is significantly larger than those prescribed in the American code (−0.3/−0.2).

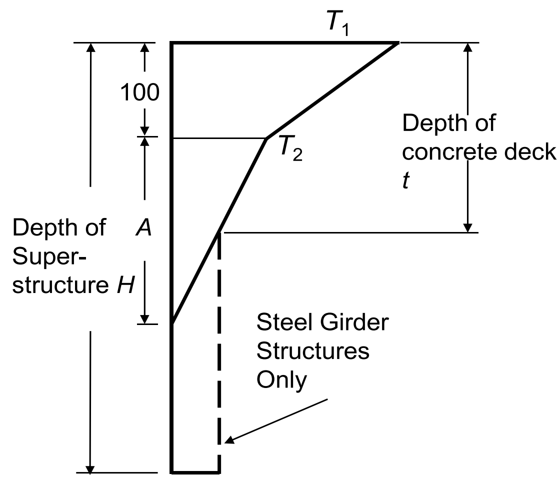

Figure 3: Vertical temperature gradient model in JTG D60 (unit: mm). Note: For concrete structures, A = 300 mm when the girder depth is greater than or equal to 400 mm; $A = H - 100$ mm when the girder depth is less than 400 mm. For steel structures with a concrete deck, A = 300 mm, where t is the thickness (in mm) of the concrete deck.

Table 8: Temperature basis for vertical solar positive temperature difference in Chinese code.

Type of Structure	T_1 (°C)	T_2 (°C)
Cement concrete pavement	25	6.7
50-mm-thick asphalt concrete pavement	20	6.7
100-mm-thick asphalt concrete pavement	14	5.5

(3) Chinese Code (TB 10002)

Unlike the highway code (JTG D60), which applies a unified climate-zone approach, the railway code (TB 10002) provides distinct, material-specific provisions. For steel members, TB 10002 mandates the use of historical extreme highest and lowest temperatures to determine thermal actions. For concrete girders, instead of the simplified multi-linear gradient model adopted in JTG D60, the railway code stipulates that the vertical temperature gradient should follow TB 10092. Based on theoretical foundations, TB 10092 employs a continuous exponential envelope curve, $T_y = T_0 e^{-ay}$, to describe the temperature distribution at the top of concrete box girders (Fig. 4). Although this represents a conservative bounding state, it ensures safety. Here, T_0 is the temperature difference along the girder height, and the parameter a varies with the structural form, orientation, and calculation time.

(4) New Zealand Code (NZTA)

This code classifies the vertical temperature gradient according to cross-sectional shape, as shown in Fig. 5. For non-box sections (e.g., T-beams, solid slab girders), it adopts a fifth-order parabolic distribution derived from the analytical solution of the one-dimensional heat conduction equation. For box sections, the gradient is simplified to a linearly decreasing distribution from the top slab downward.

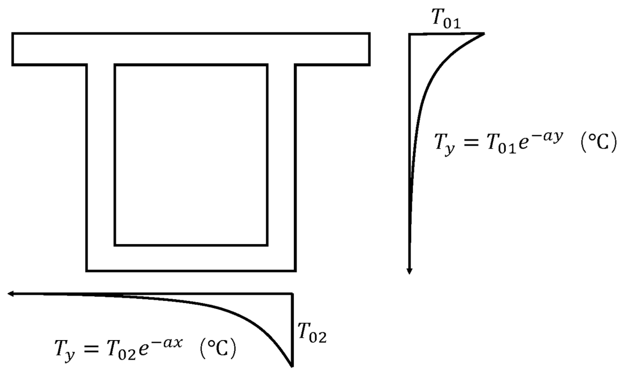

Figure 4: Vertical temperature gradient model in TB 10002 (unit: mm).

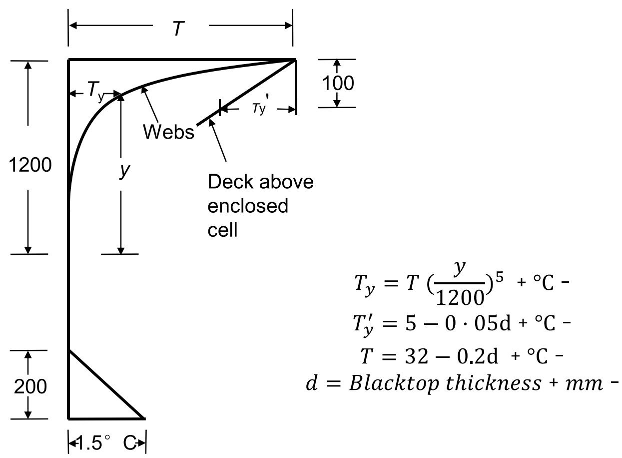

Figure 5: Vertical temperature gradient model in New Zealand code (unit: mm).

(5) Japanese Code (JSHB)

This code simplifies the calculation by omitting detailed vertical temperature gradients and using the temperature difference between structural members as the governing parameter. It assumes a uniform temperature within each member, considering only the relative temperature differences between them. The specified values are as follows: 15°C between steel members; 10°C between the concrete slab and the steel girder in composite girders; and 5°C between the top/bottom slab and the web (or rib) in concrete structures.

(6) European Code (EN 1991-1-5)

The code classifies the calculation of vertical temperature gradients into two categories: the linear simplified method and the non-linear refined method.

The linear simplified method applies to ordinary bridges. It simplifies the gradient to a linear temperature difference between the top and bottom surfaces, facilitating rapid manual calculations, as specified in Table 9.

The non-linear refined method provides detailed vertical temperature gradient profiles. It considers the temperature attenuation functions for different types of bridge structures and specifies the non-linear gradient distribution under negative temperature difference conditions, as shown in Fig. 6.

Table 9: Recommended values of linear temperature difference component in Eurocode.

Type of Deck	Top Warmer than Bottom	Bottom Warmer than Top
	ΔT_M, Heat (°C)	**ΔT_M, Cool (°C)**
Type 1: steel deck	18	13
Type 2: composite deck	15	18
Type 3: concrete deck		
Concrete box girder	10	5
Concrete beam	15	8
Concrete slab	15	8

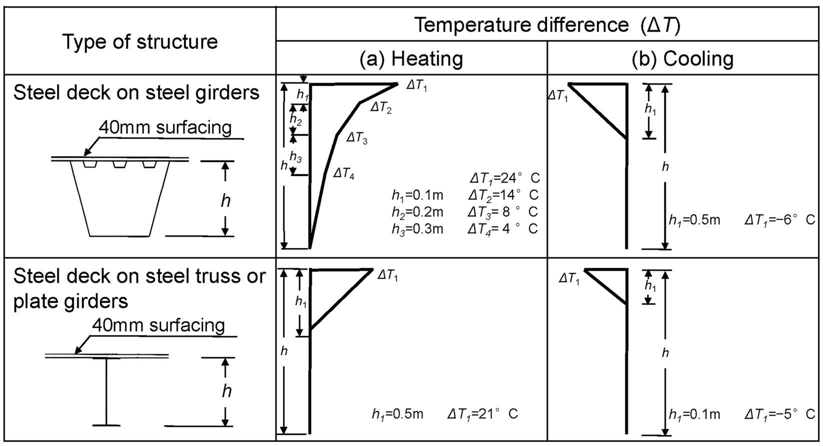

(a) Type 1: steel decks

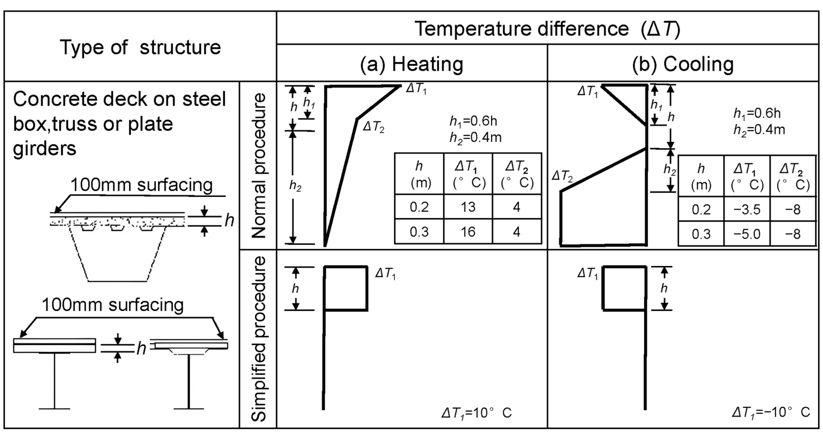

(b) Type 2: composite decks

Figure 6: (Continued)

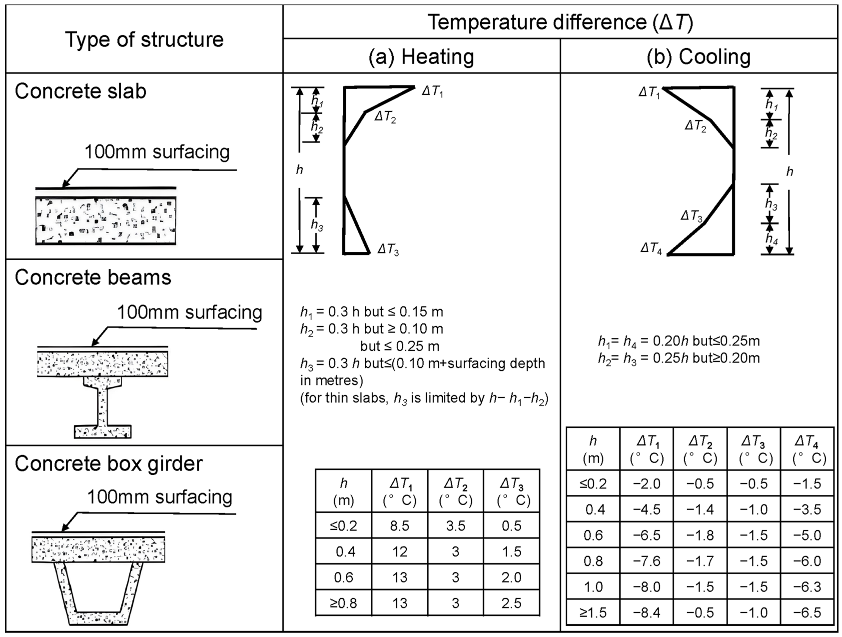

(c) Type 3: concrete decks

Figure 6: Non-linear vertical temperature gradient parameters in Eurocode.

(7) Hong Kong Code (SDM)

This code follows the core framework of the British Standard (BS EN 1991-1-5) for the vertical temperature gradient. However, in detailed calculations, the code mandates the use of a more rigorous non-linear higher-order curve model, as illustrated in Fig. 7. This attention to computational precision reflects the code's emphasis on accurately capturing temperature actions in bridge structures.

(8) Comprehensive Comparison of Vertical Temperature Gradients

To provide an intuitive visual comparison of the underlying physical and engineering assumptions regarding vertical temperature gradient models, a comprehensive comparison is conducted using a standard 2000-mm-deep concrete box girder with a 100-mm-thick asphalt overlay. As illustrated in Fig. 8, the analysis yields the following significant conclusions:

First, there is a fundamental discrepancy regarding the influence depth of the upper temperature gradient. Based on one-dimensional transient heat conduction, the New Zealand code (NZTA) assumes deep heat penetration, resulting in an influence depth of 1200 mm. In contrast, AASHTO, JTG D60, EN 1991-1-5, and HK SDM presume rapid heat attenuation, diminishing to 0°C at a depth of 400 mm.

Second, regarding the peak reference temperature difference at the top surface, the American code exhibits the most severe condition. By comparison, codes in China and Europe apply more aggressive non-linear reduction factors to rigorously quantify the strong insulating and peak-shaving effects of the 100-mm-thick heavy asphalt overlay, thereby significantly reducing the calculated top temperature differences.

Finally, concerning the lower (bottom soffit) vertical temperature gradient, the NZTA, European, and Hong Kong codes establish mandatory provisions to reflect the combined thermal effects of ground radiation reflection and bottom convection, defining a 200-mm reverse temperature gradient zone. Conversely, the Chinese and American codes conservatively envelope this lower temperature difference as 0°C in routine heating scenarios, primarily because the resulting secondary internal forces from this localized effect are often negligible for standard typologies, rather than merely for calculation efficiency.

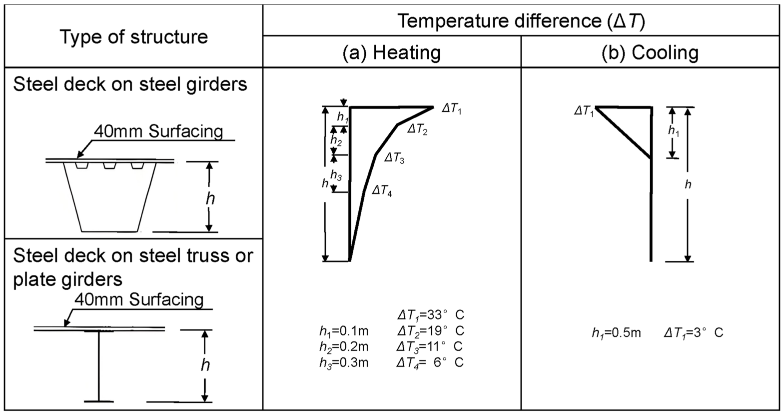

(a) Type 1: steel decks

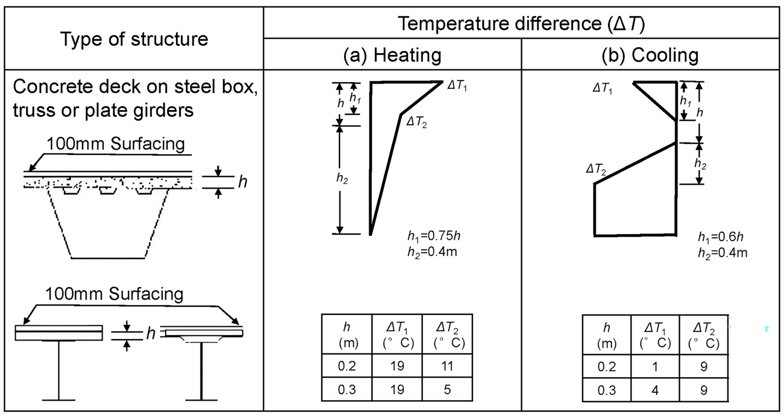

(b) Type 2: composite decks

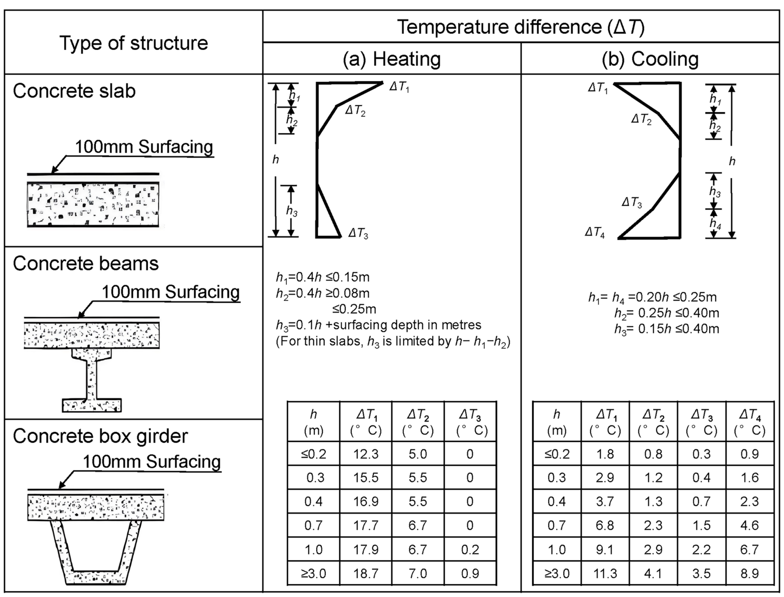

(c) Type 3: concrete decks

Figure 7: Non-linear vertical temperature gradient parameters in Hong Kong code.

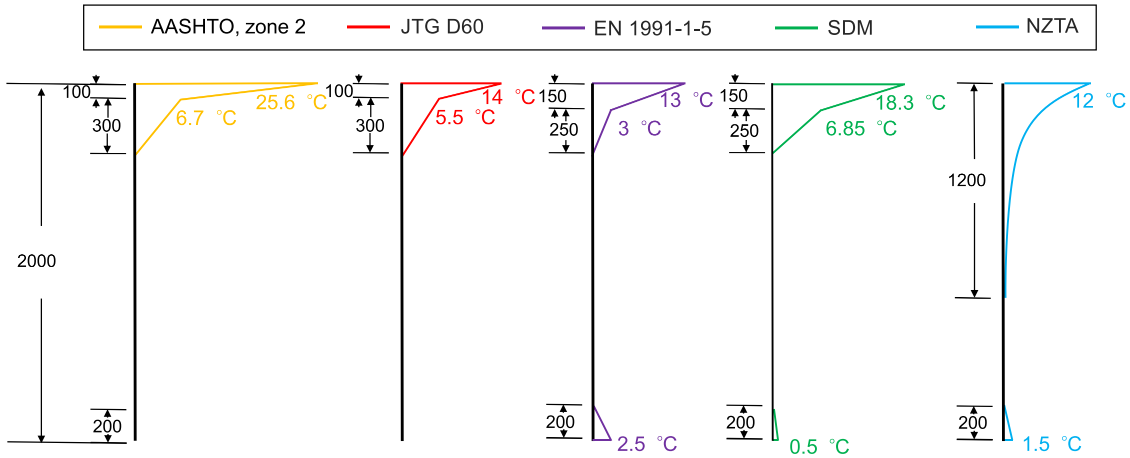

Figure 8: Comparison of vertical temperature gradients for a concrete box girder with a 100 mm asphalt overlay (unit: mm).

3.4 Combination of Uniform Temperature and Temperature Gradient Effects

The extreme values of uniform temperature depend primarily on seasonal climatic variations, whereas those of the temperature gradient result from instantaneous solar radiation, leading to significant temporal non-synchronicity between them. Consequently, national codes adopt different strategies in combining their effects.

(1) European Code (EN 1991-1-5)

This code introduces the combination coefficients $\omega_n = 0.35$ and $\omega_m = 0.75$, with the corresponding load combinations defined as follows:

Combination 1: $1.0 \times \Delta T_M$ (gradient) + $0.35 \times \Delta T_N$ (uniform)

Combination 2: $0.75 \times \Delta T_M$ (gradient) + $1.0 \times \Delta T_N$ (uniform)

(2) Hong Kong (China) Code (SDM)

This code prescribes $\omega_M = \omega_N = 1.0$, mandating the simultaneous consideration of the extreme values of both uniform temperature and temperature gradient. This approach embodies a more conservative design principle.

(3) Other Codes

Other codes do not specify dedicated internal combination coefficients within their temperature action clauses, but rather address them through the structure's general load combination procedures for the structure.

3.5 Transverse Temperature Gradient

The transverse temperature gradient is primarily induced by oblique solar radiation or the orientation of the bridge. Currently, this effect receives significantly less attention in international codes compared to the vertical temperature gradient. In most codes, it is addressed only as an advisory clause, lacking systematic provisions. In contrast, both the Chinese and European codes provide explicit consideration for this effect and specify detailed calculation methods.

(1) Chinese Code (JTG D60)

In its 2015 revision, this code supplemented provisions for the transverse temperature gradient. It emphasizes that this effect should be considered for wide box girders without cantilever slabs. The code recommends that the transverse gradient pattern be determined primarily through site-specific investigation, measurement, or analysis, based on the bridge's geographical location and environmental conditions. In the absence of measured data, the recommended transverse temperature gradient curve (Fig. 9) may be adopted. This curve is defined by the geometric relationship between the width of the outer web (B_1) and the half-width of the box girder (B), with corresponding design values provided in Table 10.

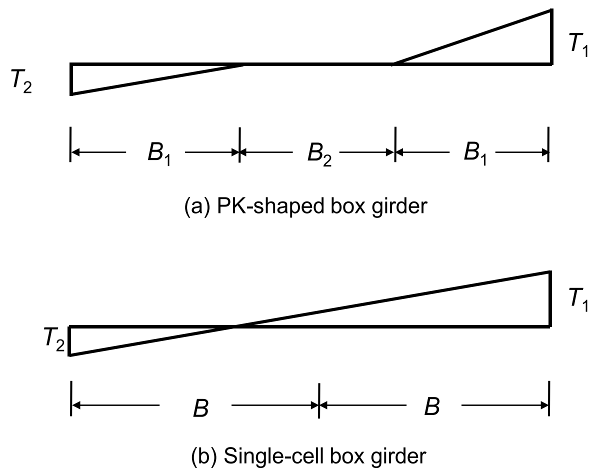

Figure 9: Calculation model for transverse temperature gradient in Chinese code.

Table 10: Transverse temperature gradient values in Chinese code.

Type of Structure	T_1 (°C)	T_2 (°C)
Concrete box girder	4.0	−2.75
Steel box girder	3.0	−1.5

(2) European Code (EN 1991-1-5)

This code recommends adopting a linear temperature difference of 5°C between opposite webs. Although this represents a simplified prescribed value, it is sufficient to satisfy design safety requirements under common service conditions.

3.6 Temperature Actions on Substructure

Bridge substructures, such as piers and pylons, also develop thermal stresses due to solar radiation and ambient temperature variations, particularly in tall or hollow piers. While national design codes primarily focus on thermal effects in the superstructure (main girders), they often lack explicit calculation rules for temperature gradients in ancillary structures like piers. In contrast, both the Chinese and European codes explicitly require the consideration of local temperature difference effects in piers.

(1) Chinese Code (JTG/T D65-05)

While the general code (JTG D60) does not provide detailed stipulations on this matter, the Specifications for Design of Highway Suspension Bridges (JTG/T D65-05) supplements it as follows: in the absence of site-measured data, a temperature gradient of 5°C across opposite surfaces of concrete pylons may be adopted as the design value.

(2) European Code (EN 1991-1-5)

This code specifies two distinct linear temperature difference components for local temperature difference effects in piers:

Lateral temperature difference between outer surfaces: For both hollow and solid concrete piers, the linear temperature difference between opposite outer surfaces due to solar shading—i.e., between the sun-exposed side and the shaded side—shall be considered. A value of 5°C is recommended.

Radial temperature difference through wall thickness: Specifically for hollow piers, a linear gradient through the pier wall thickness shall be considered to account for the thermal lag effect between the internal cavity and the external ambient temperature. A value of 15°C is recommended for this component.

3.7 Comparison of Temperature Actions in Chinese and International Bridge Codes

The European Code (EN 1991-1-5) establishes the most comprehensive framework, featuring a classification system with the clearest physical basis. It not only explicitly distinguishes the thermal lag effect in the effective temperature of different materials (steel, concrete, composite), but also provides refined temperature gradient models incorporating non-linear components. These models are capable of accurately characterizing heat transfer within complex cross-sections. Building on this physical framework, the Hong Kong Code (SDM) adapts parameters based on local subtropical climate data, demonstrating both sound theoretical advancement and strong regional adaptability.

In contrast, the American code (AASHTO) and the Chinese code (JTG D60) emphasize practical engineering applicability. Both codes employ linear or multi-linear temperature gradient models based on regional climatic zoning. While this approach significantly reduces the computational effort for conventional bridge design, its simplified models may underestimate the risk of residual stresses or lack accuracy when applied to structures with exceptionally deep box girders or in unique climatic environments. Notably, the American code compensates for this limitation by including "Procedure B", which provides a pathway for refined analysis in complex cases.

The Japanese code (JSHB) and the New Zealand code (NZTA) exhibit a distinct approach, adopting relatively simplified approaches using region-specific prescribed values or curve-based treatments. This simplification typically reflects considerations of each country's unique geographical context or design priorities, reflecting a balance between efficiency and safety within their specific engineering frameworks.

Fundamentally, the distinct vertical gradient shapes—such as the multi-linear models in AASHTO and JTG, and the non-linear curves in Eurocode and NZTA (e.g., a fifth-degree polynomial)—all originate from the same thermodynamic mechanism: one-dimensional transient heat conduction driven by diurnal solar radiation, surface wind convection, and concrete's high thermal inertia. However, for engineering practicality, codes adopt different levels of mathematical simplification. While Eurocode and NZTA closely fit the exact non-linear thermal penetration, AASHTO and JTG approximate this distribution using simplified linear segments to reduce computational effort while preserving the equivalent thermal bending moment.

3.8 Limitations of Current Codes and Advances in Refined Thermal Modeling

Although current structural design codes provide foundational guidelines for thermal actions, they are primarily calibrated for simple, idealized bridge typologies under generalized environmental conditions. As structural engineering advances, several inherent limitations in these standard codes have become apparent, driving a critical need for refined thermal modeling.

First, at the macro-spatial and geometric level, standard vertical temperature gradients often fail to capture the behavior of complex structural typologies. Recent studies [25] emphasize that complex systems, such as double-layer steel truss and road-rail suspension bridges, exhibit highly non-uniform temperature fields driven by the spatial complexity and intricate arrangement of their truss members. Consequently, applying the simplified thermal models from existing codes to these structures can introduce significant errors in predicting track alignment and structural irregularity, ultimately posing severe risks to railway operational safety. To overcome this and replace idealized boundary assumptions, refined analytical methods—such as dynamic sunlight shadow analysis and bounding box detection algorithms [26]—have proven indispensable for accurately capturing topographical shading (e.g., in mountainous areas) and the dynamic self-shading effects of these spatial truss structures.

Beyond vertical gradients in truss systems, current codes also lack sufficient granularity for non-straight geometries. They primarily address transverse temperature gradients through simplified models intended for straight bridges. However, recent studies [27] on curved steel box-girder bridges demonstrate that transverse temperature gradients exhibit a highly non-linear, Gaussian distribution rather than a simple linear profile. In curved configurations, these transverse gradients induce significant torsional moments and coupled bending-torsion effects. Relying on idealized linear differences can severely underestimate the three-dimensional thermal stress state, making it critical for future code revisions to incorporate geometry-specific transverse thermal loading models.

Similarly, at the cross-sectional level, standard design codes typically prescribe a single, unified temperature gradient for the entire bridge deck, neglecting the internal thermal complexity inherent to multi-cell (e.g., three-cell) concrete box girders [28]. The enclosed air cavities within these structures create distinct internal micro-climates, significantly altering the heat transfer process. Consequently, the temperature field of the internal middle webs differs substantially from that of the exterior side webs exposed to direct solar radiation and ambient wind. Applying a uniform gradient across the entire multi-cell cross-section fails to capture these localized thermal stresses, underscoring a strong research-driven need to explicitly incorporate internal thermodynamic boundary conditions and develop specific gradient models tailored for multi-cell configurations.

Furthermore, moving from structural geometry to external environmental boundaries, current codes predominantly rely on static, zone-based models that define temperature actions independent of the structure's global orientation. Bridge orientation is a critical determinant of solar radiation absorption, dictating the intensity and duration of thermal exposure. State-of-the-art research [29] has demonstrated that neglecting orientation-specific loading leads to severe inaccuracies. To address this, recent studies increasingly employ dynamic view factor algorithms to precisely trace ground shadows and account for the continuous spatial-temporal variations in the solar trajectory. Consequently, mainstream standards must transition from rigid regional parameterization toward refined, orientation-sensitive thermal boundary conditions.

While addressing these complex actions is crucial, another limitation lies in the evaluation phase: current codes primarily define environmental "actions" but leave "responses" entirely to numerical analysis. While finite element methods are robust, they are often computationally intensive for preliminary design or rapid condition assessments. An increasing body of research has developed simplified, closed-form analytical formulas to directly calculate temperature-induced deformations, such as mid-span deflections of continuous beams or sag variations of suspension cables [30,31]. Incorporating such analytical tools into the appendices of future codes would effectively bridge the gap between load definition and response evaluation, providing practicing engineers with reliable methods for rapid assessments.

Finally, regarding temporal variability, current codes rely heavily on historical meteorological data to define static thermal actions. This static approach inherently ignores the dynamic variability of localized temperatures and the non-stationary nature of ongoing climate change. With the rapid development of Structural Health Monitoring (SHM) systems, continuous, real-time temperature data from actual bridge sites are now readily accessible. To bridge the gap between idealized design values and actual in-service conditions, future frameworks should incorporate data-driven updating mechanisms. By employing probabilistic methods—such as Bayesian inference or non-stationary Extreme Value Theory (EVT)—engineers can continuously calibrate static design envelopes using real-time SHM data [2,32]. This paradigm shift from static reference values toward dynamic, site-specific thermal baselines is essential for proactive maintenance and accurate life-cycle performance assessments in a rapidly changing climate.

4 Temperature Actions on Tower Structures

With the development of super-long-span suspension bridges and super-tall buildings, thermal effects on pylons and high-rise tower structures have become increasingly prominent. This section focuses exclusively on temperature actions induced by the external environment; effects caused by internal industrial heat sources are not considered.

(1) Chinese Code (GB 50135)

This code specifies that the temperature difference between sun-exposed and shaded surfaces caused by solar radiation shall be based on measured data. Where such data are unavailable, a value of not less than 20°C shall be used.

(2) European Code (EN 1991-1-5)

For high-rise structures such as industrial chimneys, pipelines, silos, tanks, and cooling towers, this code establishes a systematic temperature distribution model. The temperature action is decomposed into three components: a uniform circumferential temperature component; a stepped temperature component round the circumference; and a linear temperature difference component between the inner and the outer surfaces of the wall. These components correspond respectively to the overall expansion and contraction of the tower, non-uniform circumferential stresses, and radial gradient effects, as illustrated in Fig. 10.

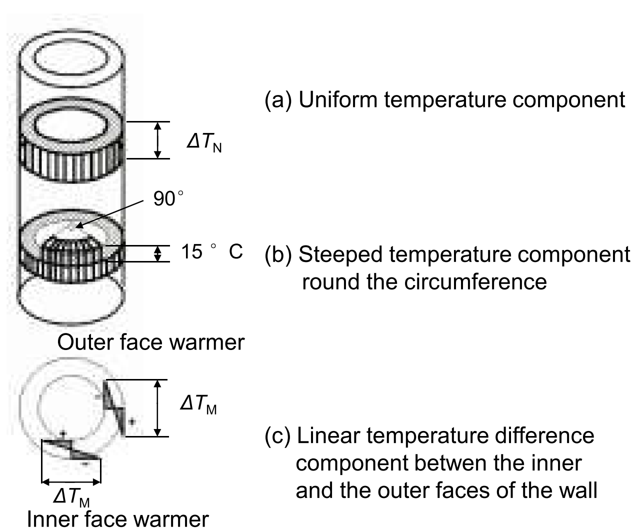

Figure 10: Temperature distribution model for chimney structures in Eurocode.

Uniform circumferential temperature component: This represents the mean temperature change governing overall expansion and contraction. The maximum and minimum uniform temperatures are taken as the maximum and minimum shade air temperatures, respectively.

Stepped temperature component round the circumference: This primarily describes the temperature non-uniformity around the cross-section induced by one-sided solar radiation. The code recommends dividing the circumference into heated shaded quadrants. For concrete structures, a stepped temperature difference of 15°C is recommended. For steel structures, the value should be determined based on specific service conditions.

Linear temperature difference component between the inner and the outer faces of the wall: This describes the linear temperature difference across the wall thickness. Owing to the low thermal conductivity and considerable thickness of concrete, a pronounced linear temperature gradient develops under rapid air temperature changes or solar exposure, for which a value of 15°C is recommended. For thin-walled steel towers without internal lining, this component can generally be neglected due to the high thermal conductivity and minimal wall thickness of steel.

5 Temperature Actions on Steel Structures

Owing to their favorable strength-to-weight ratio, steel structures are widely used in long-span spatial structures such as stadiums and airport terminals, as well as in special high-rise structures like wind-turbine towers. However, the high thermal conductivity and typically thin-walled sections of steel members render these structures sensitive to ambient temperature variations. Under complex conditions such as partial solar shading, moving shadows, or rapid transient heating, a severe non-uniform temperature field can readily develop, inducing significant secondary thermal stresses and deformations. Consequently, design codes across different engineering sectors adopt varied control strategies to address these effects.

5.1 Conventional Building Steel Structures

The Chinese code (GB 50017) specifies that the effects of thermal actions should first be mitigated through rational structural layout, such as the provision of expansion joints. The code uses the maximum length of temperature sections as the control criterion, with values given in Table 11. Thermal stress calculations or the addition of expansion joints is only mandatory when the structural length exceeds the tabulated value.

5.2 Steel-Concrete Composite Structures

Steel-concrete composite structures, which combine the advantages of both materials, are widely used in bridges. The commentary of the Chinese Standard for Design of Steel Structures (GB 50017-2017) explains the unique thermal action mechanism in such structures based on their differing thermal properties. Although the coefficients of thermal expansion of steel and concrete are similar, allowing essentially compatible deformation under uniform temperature changes, the thermal conductivity of steel is about 50 times that of concrete. Consequently, steel responds rapidly to abrupt ambient temperature changes, while concrete exhibits a pronounced thermal lag effect. The resulting temperature difference induces thermal stresses within the composite system. In simply supported beams, this leads to deflection and stress redistribution; in continuous or other statically indeterminate systems, it triggers significant secondary bending moments and restraint forces.

For exposed environments, the code recommends neglecting internal temperature gradients within the individual steel and concrete components and adopting a design temperature difference between them of 10°C to 15°C.

Table 11: Maximum length of temperature sections in Chinese code (m).

Type of Structure	Longitudinal Temperature Segment (Perpendicular to the Span Direction of the Roof Truss or Frame)	Transverse Temperature Segment (Along the Span Direction of the Roof Truss or Frame)	
		Column Top Rigid Connection	Column Top Hinged Connection
Heated buildings and buildings in non-heating regions	220	120	150
Hot workshops and unheated buildings in heating regions	180	100	125
Exposed structures	120	/	/
Buildings with profiled metal sheeting as components	250	150	

However, a simplified uniform temperature difference is insufficient for composite bridges. The severe thermal lag between the concrete deck and steel girder induces significant differential longitudinal movements, which directly dictates the shear demand on interface studs. To address this, Eurocode 4 strictly mandates that shear connectors must be designed to resist the longitudinal shear forces induced by combined thermal gradients and concrete shrinkage. Similarly, the AASHTO LRFD prescribes a distinct vertical temperature gradient model for composite girders that extends the temperature differential by 300 mm (12.0 in) down into the steel section. Furthermore, to prevent premature stud fatigue under these superimposed longitudinal forces, AASHTO requires shear connectors to be distributed throughout the entire length of continuous composite bridges.

5.3 Limitations of Existing Codes

The emergence of new steel structural forms has revealed a significant lag in the provisions for temperature actions in current codes. Owing to the high thermal conductivity of steel, these structures are extremely sensitive to solar radiation, where complex mutual shading effects among members can readily induce severe non-linear transient temperature gradients. However, prevailing codes, such as GB 50017, primarily focus on mitigating global uniform temperature differences by limiting temperature segment lengths. They lack refined calculation models for temperature gradient applicable at either the member cross-section or global structural level. Consequently, in the absence of a unified industry benchmark, designers often must rely on numerical simulations or physical tests to determine design parameters. Given the increasing prevalence of steel and steel-concrete composite structures in modern infrastructure, developing a refined thermal loading system that accounts for their unique thermal properties represents a critical challenge for future code revisions.

6 Comparison of Partial Safety Factors and Limit States

Within the limit state design framework, temperature actions are categorized as deformation-induced indirect actions. The magnitude of their effects depends not only on the characteristic temperature difference but is also directly governed by the values assigned to partial safety factors and combination coefficients. Owing to different reliability-based design criteria and varying interpretations of the stiffness degradation mechanism in concrete after cracking, national codes exhibit significant discrepancies in the values of these partial factors, as compared in Table 12.

Table 12: Comparison of partial safety factors and combination coefficients for temperature actions in codes.

Limit States	Country	Type of Structures	Partial Safety Factors	Combination Coefficients
Ultimate limit states (ULS)	China	Building structures GB 50009	1.4	0.6
		Bridge structures JTG D60	1.4	0.8
	Europe	General purpose EN 1990/1991	1.5	0.6
	America	Bridge structures AASHTO	Deformation: 1.2 Force effect: 0.5	
Serviceability limit states (SLS)	Common to all national codes	All kinds of structures	1.0	1.0

6.1 Ultimate Limit States

(1) Chinese Codes

In both the building structures code (GB 50009) and the bridge design code (JTG D60), the partial safety factor for temperature actions is taken as 1.4. However, a subtle difference exists in their load combination rules. For building structures, a combination coefficient of 0.6 is applied to temperature actions, reflecting the extremely low probability of the simultaneous occurrence of extreme temperatures with extreme wind or snow loads. In contrast, bridge structures are directly exposed to the environment and are more susceptible to climatic influences. Consequently, when temperature actions are combined with vehicle loads (where temperature is considered a secondary action), a combination coefficient of 0.8 is used. This higher value reflects the greater emphasis placed on the environmental sensitivity of bridge structures.

(2) European Code (EN 1990)

This code specifies a partial safety factor of 1.5 and a combination coefficient of 0.6 for temperature actions. Given that natural environmental actions such as temperature and wind load exhibit greater statistical variability and uncertainty compared to the most stable permanent loads, a higher partial safety factor is assigned to variable actions. This approach ensures that the overall structure satisfies the predefined target reliability index.

(3) American Code (AASHTO)

A partial safety factor of 1.2 is applied when verifying deformations of expansion joints and bearings to ensure detailing safety. Conversely, for calculating secondary internal forces in the structure, which accounts for the stiffness reduction and stress relaxation due to concrete cracking and creep, a factor of only 0.5 is used under ultimate limit states (ULS).

6.2 Serviceability Limit States

A consensus is observed among national codes regarding serviceability limit states, which address crack control and deformation verification. As these states pertain to structural performance under ordinary service conditions rather than resistance to ultimate failure, the partial safety factor for temperature actions is commonly set to 1.0.

7 Conclusions

Based on a systematic comparative study of temperature actions in the structural design codes of China, the United States, Europe, Japan, New Zealand, and Hong Kong (China), the following conclusions are drawn:

(1) Differences in calculation models: The American and Chinese codes emphasize simplified calculation approaches based on meteorological statistics and engineering experience, prioritizing practical application. The European code establishes a more rigorous theoretical framework incorporating material thermal properties, structural geometry, and refined temperature gradient models. The New Zealand code adopts a minimalist prescribed-value method, suited to its temperate climate. The Japanese code utilizes a simplified inter-member temperature difference model, reflecting a unique balance between computational efficiency and practicality within its high-seismicity context. The Hong Kong code has successfully implemented localized adaptations of the European framework.

(2) Differences in safety margins: Under ultimate limit states (ULS), the Chinese and European codes assign higher partial safety factors (1.4 to 1.5) to temperature actions, treating them as external forces to be resisted through structural stiffness. In contrast, the American code adopts lower factors (0.5 to 1.2), recognizing the self-limiting nature of temperature actions and reflecting a design philosophy that utilizes structural resilience to accommodate deformation-induced loads.

(3) Urgency of code updates: The intensification of global warming has increased the frequency of extreme temperature events, potentially rendering design bases reliant on historical statistical data unsafe. The proactive increase of design temperature differences in the Hong Kong (China) code (2023 edition) offers a critical warning for other national codes. It is recommended that future revisions of Chinese codes proactively address climate change trends by incorporating adaptive adjustments to the characteristic values of base temperatures and effective temperatures, thereby ensuring the safety of infrastructure throughout its entire service life.

(4) Recommendations for code revision: Given China's vast territory and diverse climatic conditions, the region-specific simplified or prescribed-value methods used in the Japanese and New Zealand codes are not universally applicable. In contrast, the European code has established a comprehensive physical framework covering buildings, bridges, and tower structures, which offers a valuable reference. While the substantial upward revision of the design temperature differences in the Hong Kong code demonstrates foresight in addressing climate change, it is imperative to note that China's current major codes (e.g., GB 50009, JTG D60) were issued over a decade ago and urgently require adaptive revisions.

Acknowledgement: The authors would like to thank the editors and reviewers for their valuable comments and suggestions, and also express sincere gratitude to Professor Yuhong Ling for his professional guidance and support throughout the research process.

Funding Statement: This research was funded by the financial support from the National Natural Science Foundation of China (Nos. 52078220 and 52578364).

Author Contributions: Linren Zhou: Conceptualization, Supervision, Writing—review and editing. Zhibo Xie: Methodology, Data curation, Writing—original draft. Jingyi Huang: Formal analysis, Investigation, Writing—original draft. All authors reviewed and approved the final version of the manuscript.

Availability of Data and Materials: The authors confirm that the data supporting the findings of this study are available within the article.

Ethics Approval: Not applicable.

Conflicts of Interest: The authors declare no conflicts of interest.

References

1. World Meteorological Organization. State of the global climate 2024. Geneva, Switzerland: WMO; 2025.
2. Li L, Chen B, Zhou L, Xia Q, Zhou Y, Zhou X, et al. Thermal behaviors of bridges—a literature review. Adv Struct Eng. 2023;26(6):985–1010. doi:10.1177/13694332231153976.
3. Zhang L, Wang X, Wang F, Ni P, Zhou X, Xia Y. Impact of climate change on the thermal behavior of long-span suspension bridges. J Bridge Eng. 2026;31(3):04025109. doi:10.1061/jbenf2.beeng-7581.
4. Li Y, Huang X, Zhu J. Research on temperature effect on reinforced concrete bridge pylon during strong cooling weather event. Eng Struct. 2022;273(10):115061. doi:10.1016/j.engstruct.2022.115061.
5. Li S, Chen S. Field monitoring and prediction on temperature distribution of glass curtain walls of a super high-rise building. Eng Struct. 2022;250(5):113405. doi:10.1016/j.engstruct.2021.113405.
6. Xu W, Chen D, Qian H. Non-uniform temperature fields and effects of steel structures: review and outlook. Appl Sci. 2020;10(15):5255. doi:10.3390/app10155255.
7. Zhou L, Xie Z, Fan Y, Shan Y, Koo KY, Xia Y. Spatial characteristics of temperature effects on a long-span steel box girder suspension Bridge. Adv Struct Eng. 2025;28(15):2893–909. doi:10.1177/13694332251365972.
8. Shen Q, Chen J, Yue C, Cao H, Chen C, Qian W. Investigation on the through-thickness temperature gradient and thermal stress of concrete box girders. Buildings. 2023;13(11):2882. doi:10.3390/buildings13112882.
9. Zhao L, Zhou LY, Zhang GC, Wei TY, Mahunon AD, Jiang LQ, et al. Experimental study of the temperature distribution in CRTS-II ballastless tracks on a high-speed railway bridge. Appl Sci. 2020;10(6):1980. doi:10.3390/app10061980.
10. Huang W, Meng X, Xu W, Mei M, Yao X, Chen F, et al. Study of thermal effects on large-span ring-shaped steel structures. Buildings. 2025;15(21):3822. doi:10.3390/buildings15213822.
11. Hu D, Sun Q, Xie K, Yan B. Vertical temperature gradient test and numerical simulation of steel box girders in cold regions. J Perform Constr Facil. 2023;37(2):04023009. doi:10.1061/jpcfev.cfeng-4212.
12. Cai C, Huang S, He X, Zhou T, Zou Y. Investigation of concrete box girder positive temperature gradient patterns considering different climatic regions. Structures. 2022;35(8):591–607. doi:10.1016/j.istruc.2021.11.030.
13. Zhang L, Wang X, Chen ZP, Qiang J, Xia Y. Climate change intensifies bridge temperature: evidence from 26 Years of monitoring data. Adv Struct Eng. 2026;29(6):1202–13. doi:10.1177/13694332251377551.
14. GB 50009-2012. Load code for the design of building structures. Beijing, China: China Architecture & Building Press; 2012. (In Chinese).
15. JTG D60-2015. General specifications for design of highway bridges and culverts. Beijing, China: China Communications Press; 2015. (In Chinese).
16. EN 1991-1-5:2003. Eurocode 1: actions on structures—part 1–5: general actions—thermal actions. Brussels, Belgium: CEN; 2003.
17. American Association of State Highway and Transportation Officials. LRFD bridge design specifications. 10th ed. Washington, DC, USA: AASHTO; 2024.
18. Highways Department of Hong Kong. Structures design manual for highways and railways (2013 Edition, 2025 Revision). Hong Kong, China: Highways Department; 2025.
19. JTG/T D65-05-2015. Specifications for design of highway suspension bridges. Beijing, China: China Communications Press; 2015. (In Chinese).
20. GB 50135-2019. Standard for design of high-rising structures. Beijing, China: China Architecture & Building Press; 2019. (In Chinese).
21. GB 50017-2017. Standard for design of steel structures. Beijing, China: China Architecture & Building Press; 2017. (In Chinese).
22. TB 10002-2017. Code for design on railway bridge and culvert. Beijing, China: China Railway Publishing House; 2017. (In Chinese).

23. NZ Transport Agency. Bridge manual (SP/M/022). 3rd ed. Wellington, New Zealand: NZ Transport Agency; 2013.
24. Japan Road Association. Specifications for highway bridges (JSHB). Tokyo, Japan: Japan Road Association; 2017.
25. Zhu Y, Sun D, Shuang M. Investigation of temperature-induced effect on rail-road suspension bridges during operation. J Constr Steel Res. 2024;215(6):108542. doi:10.1016/j.jcsr.2024.108542.
26. Zhu Y, Sun D, Guo H, Shuang M. Fine analysis for non-uniform temperature field and effect of railway truss suspension bridge under solar radiation. J Constr Steel Res. 2023;210(6):108098. doi:10.1016/j.jcsr.2023.108098.
27. Cui F, Zhang X, Li H, Elghazouli AY, Liu Y. Temperature field effects and thermal-induced response of curved steel box-girder bridges using field monitoring data and numerical assessments. J Constr Steel Res. 2026;237(6):110102. doi:10.1016/j.jcsr.2025.110102.
28. Zhang F, Han HZ, Yu Y, Wang CS, Xu S. Testing and analysis of temperature field in a three-cell concrete box girder model. J Bridge Eng. 2026;31(2):04025104. doi:10.1061/jbenf2.beeng-7749.
29. Wang A, Zhang Z, Lei X, Xia Y, Sun L. All-weather thermal simulation methods for concrete maglev bridge based on structural and meteorological monitoring data. Sensors. 2021;21(17):5789. doi:10.3390/s21175789.
30. Zhou Y, Xia Y, Chen B, Fujino Y. Analytical solution to temperature-induced deformation of suspension bridges. Mech Syst Signal Process. 2020;139(3):106568. doi:10.1016/j.ymssp.2019.106568.
31. Zhou Y, Xia Y, Fujino Y. Analytical formulas of beam deflection due to vertical temperature difference. Eng Struct. 2021;240:112366. doi:10.1016/j.engstruct.2021.112366.
32. Yang DH, Guan ZX, Yi TH, Li HN, Liu H. Structural temperature gradient evaluation based on bridge monitoring data extended by historical meteorological data. Struct Health Monit. 2024;23(3):1800–15. doi:10.1177/14759217231184276.